Note: Fully integrated active quenching circuit achieving 100 MHz count rate with custom technology single photon avalanche diodes

G. Acconcia, I. Labanca, I. Rech, A. Gulinatti, and M. Ghioni

Citation: Review of Scientific Instruments **88**, 026103 (2017); doi: 10.1063/1.4975598

View online: http://dx.doi.org/10.1063/1.4975598

View Table of Contents: http://aip.scitation.org/toc/rsi/88/2

Published by the American Institute of Physics

REVIEW OF SCIENTIFIC INSTRUMENTS **88**, 026103 (2017)

Note: Fully integrated active quenching circuit achieving 100 MHz count rate with custom technology single photon avalanche diodes

G. Acconcia,[a)] I. Labanca, I. Rech, A. Gulinatti, and M. Ghioni
Dipartimento di Elettronica, Informazione e Bioingegneria, Politecnico di Milano, Piazza L. da Vinci 32, 20133 Milan, Italy

(Received 16 December 2016; accepted 23 January 2017; published online 6 February 2017)

The minimization of Single Photon Avalanche Diodes (SPADs) dead time is a key factor to speed up photon counting and timing measurements. We present a fully integrated Active Quenching Circuit (AQC) able to provide a count rate as high as 100 MHz with custom technology SPAD detectors. The AQC can also operate the new red enhanced SPAD and provide the timing information with a timing jitter Full Width at Half Maximum (FWHM) as low as 160 ps. *Published by AIP Publishing.* [http://dx.doi.org/10.1063/1.4975598]

Single Photon Avalanche Diodes (SPADs) have gained a prominent role in the measurement of optical signals, driven by the need for ultimate sensitivity in various scientific and industrial applications such as Förster Resonance Energy Transfer (FRET)[1] and Single Molecule Fluorescence Spectroscopy (SMFS)[2] in life sciences, Quantum Key Distribution (QKD)[3] in cryptography and communication, and Laser Imaging Detection and Ranging (LIDAR)[4] in remote objects sensing.

Best in class results in terms of SPAD Photon Detection Efficiency (PDE), particularly at the wavelengths of interest in biological applications, and Dark Count Rate (DCR) even with large active areas up to 500 μm have been obtained resorting to technologies specifically developed for SPAD fabrication,[5] usually referred to as *custom* technologies. A significant breakthrough in this field is represented by the recently developed Red Enhanced SPAD (RE-SPAD),[6] able to provide a PDE as high as 40% at a wavelength of 800 nm and fabricated with a planar fabrication process that makes it feasible to develop SPAD arrays particularly suited for demanding applications in the field of life sciences.

In order to obtain very high performance with custom technology SPAD detectors, an external Active Quenching Circuit (AQC) designed on purpose is necessary.

AQC characteristics significantly contribute to determine the detector performance:[7] a prompt quenching of the SPAD avalanche current has beneficial effects on power consumption and afterpulsing probability[7] and a short dead time is a key parameter to achieve high counting efficiency.[8]

The exploitation of standard CMOS technologies for the fabrication of the SPAD detector and the quenching electronics on the same chip opened the way to the development of detection systems featuring a dead time of a few nanoseconds.[9,10] This approach, though, is limited by the fact that the detector is fabricated using structures (i.e., tubs and wells) that have been designed to optimize transistors performance; as a result, the PDE in the near-infrared region of the spectrum is usually limited to a few percent due to the small depth of carrier collection layers while the high electric fields arising from higher doping result in a strongly enhanced DCR due to band-to-band and trap-assisted tunneling effects. Recently, other solutions including extra layers in the standard CMOS fabrication process,[11] back-illumination,[12] and high bias voltage for the detector[13] have been investigated in order to increase the sensitivity of CMOS SPADs at wavelengths above 700 nm. Nevertheless, the overall performance of these solutions is still mainly limited by the constraints imposed by the use of a single technology for both the detector and the electronics.

On the other hand, the exploitation of custom technology SPAD detectors requires quenching pulses with an amplitude ranging from a few volts for SPADs fabricated with standard custom technology to tens of volts for RE-SPADs[6] and the parasitics due the external connection between the detector and the external AQC set tight constraints in determining the system speed.

In this paper, we present a fully integrated active quenching circuit able to operate custom technology SPAD detectors with a dead time as low as 10 ns. Being able to apply quenching pulses up to 50 V, the circuit can properly operate RE-SPADs and extract the timing information with a timing jitter as low as 160 ps.

The AQC has the same structure reported in Ref. 14, it is based on three main blocks: the sense stage that promptly senses the avalanche current onset and passively quenches it, the high-side logic block that drives the high-voltage MOSFET that actively completes the quenching operation, and the low-side logic block that controls the proper operation of the whole circuit and drives the high-voltage MOSFET that performs the reset of the SPAD detector.

The circuit features the capability to apply quenching pulses with an amplitude up to 50 V, thanks to the exploitation of high-voltage transistors for quench and reset phases, while low voltage devices have been exploited in order to achieve a high operating speed. In this work, we demonstrated that it is possible to boost the count rate of this structure up to the

[a)]Author to whom correspondence should be addressed. Electronic mail: giulia.acconcia@polimi.it.

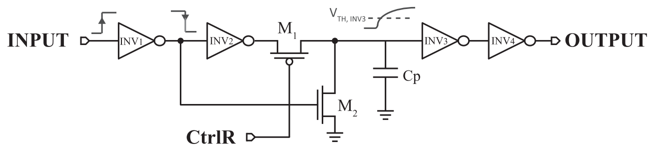

FIG. 1. Schematic of the programmable delayer circuit that sets the duration of the reset phase.

remarkable value of 100 MHz, with an improvement factor of 25% with respect to Ref. 14. In particular, we reduced the contribution of the programmable delayer to the overall duration of the reset phase by increasing the aspect ratio of the p-type MOSFET M_1 (see Fig. 1) up to 400 nm/180 nm; in this way, with CtrlR equal to 0 V, the minimum duration of the reset phase can be set lower than 4 ns. To the best of our knowledge, the presented circuit is the first fully integrated AQC able to drive custom technology SPAD detectors at a count rate as high as 100 MHz.

With this circuit, we also proved for the first time that it is possible to extract the timing information from the new RE-SPAD using a fully integrated AQC designed on purpose.

The new AQC has been fabricated exploiting the high voltage 0.18 μm CMOS technology from Austriamicrosystems (ams H18) and extensively characterized with two different custom technology SPAD detectors. First of all, a thin 50 μm-diameter custom technology SPAD has been used in order to test the speed of the circuit because it can be properly operated with an overvoltage as low as 5 V, which is a good tradeoff between PDE and DCR performance; using a low overvoltage, indeed, is necessary to guarantee that the final value after quenching and reset phases is achieved when using a few nanoseconds for the two phases. The AQC and the SPAD have been placed on a custom PCB developed on purpose and a direct wire bonding has been used to connect the AQC to the SPAD anode terminal in order to minimize the stray capacitance and inductance associated to the connection.

The duration of the quench and reset phases has been set to their minimum values by minimizing the voltage at the external control pins CtrlR and CtrlQ that drive two programmable delayers with the structure reported in Fig. 1.

The SPAD has been illuminated with a laser diode (Antel MPL-820 laser module) emitting optical pulses at 820 nm and the waveform at the anode has been acquired with an oscilloscope, using a trigger tool of the scope that selects the pulses at the minimum distance; it is worth noting that particular attention has been used in order to make the capacitive load introduced by the setup negligible with respect to the overall SPAD, AQC, and connection capacitance. The acquired waveform is shown in Fig. 2: as can be seen, the minimum dead time is as low as 10 ns, thus making this AQC able to achieve the state-of-art count rate of 100 MHz with a custom technology thin SPAD detector. As previously said, the characteristics of the AQC strongly affect the performance of the SPAD detector. Concerning the afterpulsing probability, this is strongly affected by the amount of charge that flows through the device upon an avalanche is triggered; a fast quenching of the avalanche is fundamental in order to limit the afterpulsing. Moreover, it is worth noting that if the trapped charges are released when the SPAD is kept below the breakdown voltage, i.e., during the so-called hold-off time, no avalanche is triggered and afterpulsing is reduced. Since the presented AQC is able to operate a thin custom technology SPAD with a dead time as short as 10 ns, which implies that also the hold-off time is limited to a few nanoseconds (see Fig. 2), we evaluated the afterpulsing probability as a function of the dead-time set by the AQC. The results are reported in Fig. 3: as expected, the afterpulsing probability increases as the dead time is reduced; nevertheless, the maximum value of the total afterpulsing probability is as low as 1.8%. This result makes the use of the presented AQC with a thin SPAD detector exploiting a 10 ns dead time practically feasible in high-performance applications. The presented AQC is not only able to operate custom technology SPAD detector up to 50 V of overvoltage but it is also able to provide the timing information about the arrival time of the photon that triggered an avalanche with a good timing accuracy. In particular, in this work, we present the first timing measurement ever carried out with a RE-SPAD using a fully integrated AQC.

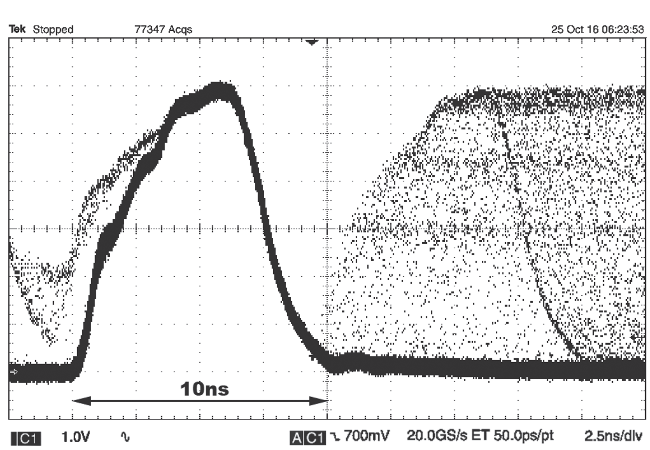

FIG. 2. Measurement of the minimum dead time between two pulses using the presented circuit and a custom technology 50 μ-diameter SPAD detector: a SPAD that has been triggered by an event is ready to detect another photon in just 10 ns with the designed AQC.

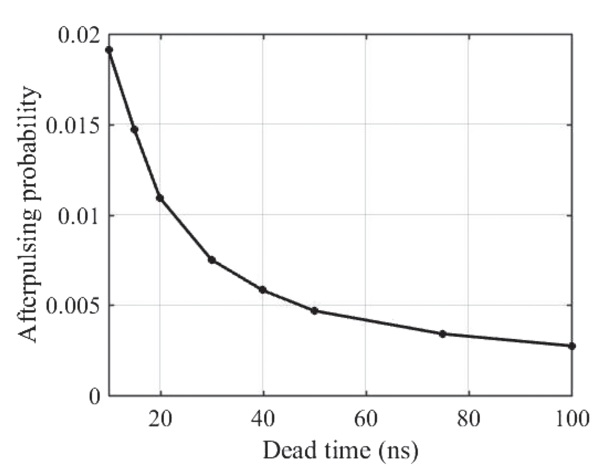

FIG. 3. Afterpulsing probability of a custom technology 50 μ-diameter SPAD detector driven by the presented AQC as a function of the dead time.

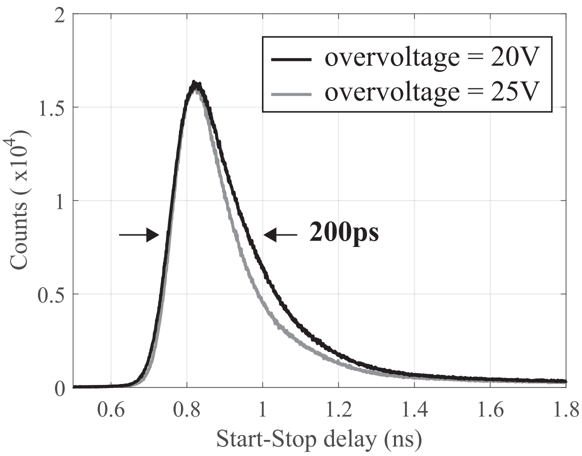

FIG. 4. Instrument response function of a RE-SPAD operated by the presented AQC at two different excess bias: the timing jitter FWHM is 200 ps at 20 V (black) and 160 ps at 25 V (gray).

The Instrument Response Functions (IRFs) of the RE-SPAD operated by the AQC at two different excess bias are reported in Fig. 4: the setup consisted of a dedicated printed circuit board for the SPAD and the AQC, a laser diode (Antel MPL-820 laser module) emitting optical pulses at 820 nm with about 10 ps Full Width at Half Maximum (FWHM), and a commercial Time Correlated Single Photon Counting (TCSPC) module (SPC-130 by Becker and Hickl). The TCSPC module receives the AQC timing output as CFD input (START) and the electrical output of the laser, which is synchronous with the optical pulse, as SYNC input (STOP). As shown in Fig. 4, the presented AQC is able to provide the timing information about a photon impinging on the RE-SPAD with a timing accuracy down to 200 ps FWHM using an overvoltage of 20 V and 160 ps with 25 V.

[1] A. Ingargiola, R. A. Colyer, D. Kim, F. Panzeri, R. Lin, A. Gulinatti, I. Rech, M. Ghioni, S. Weiss, and X. Michalet, Proc. SPIE **8228**, 82280B (2012).

[2] X. Michalet, A. Ingargiola, R. A. Colyer, G. Scalia, S. Weiss, P. Maccagnani, A. Gulinatti, I. Rech, and M. Ghioni, IEEE J. Sel. Top. Quantum Electron. **20**, 6 (2014).

[3] K. J. Gordon, V. Fernandez, P. D. Townsend, and G. S. Buller, IEEE J. Quantum Electron. **40**, 7 (2004).

[4] S. Pellegrini, G. S. Buller, J. M. Smith, A. M. Wallace, and S. Cova, Meas. Sci. Technol. **11**, 6 (2000).

[5] D. Bronzi, F. Villa, S. Tisa, A. Tosi, and F. Zappa, IEEE Sens. J. **16**, 1 (2016).

[6] A. Gulinatti, I. Rech, F. Panzeri, C. Cammi, P. Maccagnani, M. Ghioni, and S. Cova, J. Mod. Opt. **59**, 17 (2012).

[7] S. Cova, M. Ghioni, A. Lacaita, C. Samori, and F. Zappa, Appl. Opt. **35**, 12 (1996).

[8] P. Peronio, G. Acconcia, I. Rech, and M. Ghioni, Rev. Sci. Instrum. **86**, 11 (2015).

[9] C. Niclass and M. Soga, in Proceedings of IEEE International Electron Device Meeting (IEDM 2010) (IEEE, 2010).

[10] A. Eisele, R. K. Henderson, B. Schmidtke, T. Funk, L. Grant, J. Richardson, and W. Freude, in *Proceedings of International Image Sensor Workshop* (2011), pp. 278–281, available at https://pdfs.semanticscholar.org/25f0/8c55f36a73dc2cfeb7fa5a81c5e05fc10f4b.pdf.

[11] I. Takai, H. Matsubara, M. Soga, M. Ohta, M. Ogawa, and T. Yamashita, Sensors **16**, 4 (2016).

[12] J. M. Pavia, M. Scandini, S. Lindner, M. Wolf, and E. Charbon, IEEE J. Solid-State Circuits **50**, 10 (2015).

[13] E. A. Webster, L. A. Grant, and R. K. Henderson, IEEE Electron Device Lett. **33**, 11 (2012).

[14] G. Acconcia, I. Rech, A. Gulinatti, and M. Ghioni, Opt. Express **24**, 16 (2016).